



DEMAGNETIZATION ANALYSIS OF A NEW HEFSM WITH 12-SLOT 10-POLE AND 12-SLOT 14-POLE CONFIGURATIONS

Siti Khalidah Rahimi, Erwan Sulaiman, Mahyuzie

Jenal, M.Z. Ahmad, Nurul 'Ain Jafar

Research Center for Applied Electromagnetics (EMC), Universiti Tun Hussein Onn Malaysia (UTHM),
86400 Parit Raja, Batu Pahat, Johor Malaysia

E-Mail: sitikhalidah17@gmail.com, erwan@uthm.edu.my, mahyuzie@uthm.edu.my, zarafi@uthm.edu.my, aienjafar@yahoo.com

ABSTRACT

Based on the irreversible demagnetization of the permanent magnet (PM) in Hybrid Excitation Flux Switching Machine (HEFSM), the demagnetization mechanism of PM for 12-slot 10-pole and 12-slot 14-pole at various temperatures for its initial and final design are analyzed for comparison. In order to remove excessive PM demagnetization, mitigation of PM in the final design of 12-slot 10-pole and 12-slot 14-pole HEFSM with several steps is conducted. Upon removing the demagnetization area in PM, the PM size is restructured to keep the PM volume constant while keeping other parameters constant and zero demagnetization after mitigation process is achieved. It is found that PM demagnetization at the final design is reduced after several steps of optimization. The mitigation process shall also be contributed to the development of the anti-demagnetization technology for Hybrid electric vehicles (HEV).

Key words: demagnetization, permanent magnet (PM), Hybrid Excitation Flux Switching Machine (HEFSM), mitigation process, Hybrid electric vehicles (HEV).

INTRODUCTION

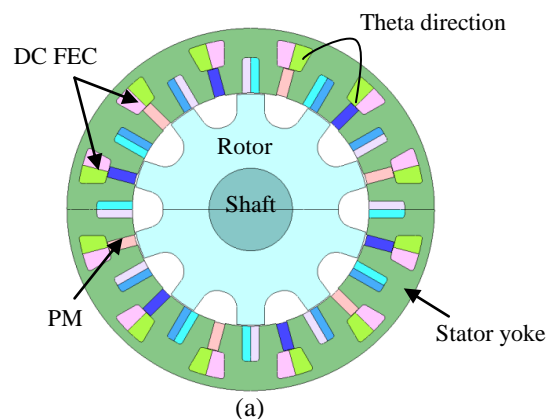
Generally, flux switching machine (FSM) can be categorized into three groups that are permanent magnet flux switching machine (PMFSM), field excitation flux switching machine (FEFSM), and hybrid excitation flux switching machine (HEFSM). Both PMFSM and FEFSM has only PM and field excitation coil (FEC), respectively as their main flux sources, while HEFSM combines both PM and FEC on the stator (E. Sulaiman, Kosaka & Nobuyuki Matsui, 2011), (S.K. Rahimi & E. Sulaiman, 2014). For PMFSM, since only PM is used as their main magnetic flux generation, the construction is more simple and easy when compared to FEFSM and HEFSM. However, the constant PM flux is difficult to control and the cost of PMFSM is also slightly higher compared to other design due to high volume of PM.

Meanwhile, FEFSM uses DC field excitation (FE) as a main flux source. The current flow through to the winding produced magnetic field when an external DC voltage is applied, makes this kind of FSM is quite complicated to design. The cost of construction is very low because do not utilize PM.

Hybrid excitation flux switching machines (HEFSMs) are those which utilize primary excitation by PMs as well as DC FEC as a secondary source. HEFSM is an alternative option where the advantages of both PM machines and DC FEC synchronous machines are combined (E. Sulaiman, M.Z. Ahmad & Kosaka, 2012). This type of FSM have potential to improve variable flux capability, power and torque density, flux weakening performance and efficiency which have been researched over many years (Y.

Amara, L. Vido & M. Gabsi, 2006), (C. Zhao & Y. Yan, 2005). As one advantage of the DC FEC, the flux of PM can easily be controlled with variable flux control capabilities. Other than that, since all active parts are located in stator, HEFSM is easy to manage magnet temperature rise and it is expected that a simple cooling system can be used for this machine (R.L. Owen, Z. Q. Zhu & G. W. Jewell, 2009).

Various combinations of stator slot and rotor pole of HEFSM have been developed for high-speed application. All previous design HEFSM have armature coil and FEC, arranged in theta direction. But the machines with theta direction have problem of flux cancellation between FEC and armature coil. In order to eliminate the flux cancellation effect in the original design, a new HEFSM having 12-slot 10-pole with FEC in radial arrangement has been proposed. The proposed design has also the characteristics of improving torque performances as compare to the machine having theta direction. Comparisons between the original design of 12-slot 10-pole HEFSM with FEC in theta direction and the proposed 12-slot-14P HEFSM with radial direction are illustrated in Figure 1.



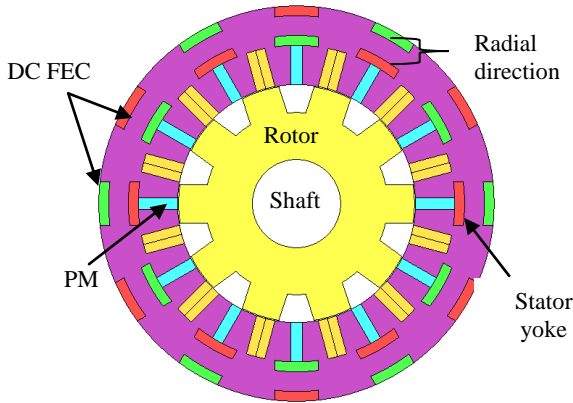


Figure 1:Original and proposed design of HEFSM (a) 12S-10P HEFSM in theta direction (b) 12S-14P HEFSM in radial direction

The arrangement of FEC located on the stator is different with previous design with FEC in theta direction. In new design, FEC wound in radial direction in which the windings is located between PM at stator outer is proposed. However the proposed FEC design limits flux movement through air gap at outer space of upper FEC. This situation will results in excessive flux leakage production the machine. Adding some layer at upper FEC can be a solution to generate more flux and reduce the flux

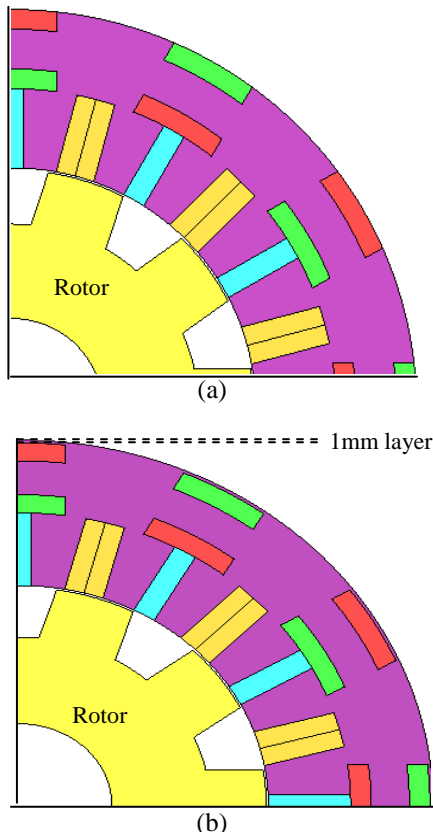


Figure 2: A structure of 12S-10P HEFSM (a) Without layer (a) With layer

loss to the surrounding. By adding 1mm layer in a stator, all parameter and position of all parts are kept constant except the position of upper FEC. Figure 2 shows the different between 12-slot 10-pole HEFSM configuration with and without layer.

Since the initial performances are not achieved the target torque and power for HEV applications of 303Nm and 123kW, respectively, design improvement is conducted by updating eight individual parameters identified as P1 to P8 by using ‘Deterministic Optimization Method’ (DOM). Eight design parameters which is sensitive towards the improvement of machine performance are defined in rotor and stator part. The method is treated repeatedly by changing P1 to P8 until the target maximum torque and power are achieved (E.Sulaiaman, T. Kosaka & N.Matsui, 2011). In addition, the main machine dimensions of final design for both 12-slot 10-pole and 12-slot 14-pole HEFSM which meet the optimum torque and power are illustrated in Figure 3. Finally, the overall performances of the final design of 12-slot 10-pole and 12slot 14-pole HEFSM are summarized in Table 1.

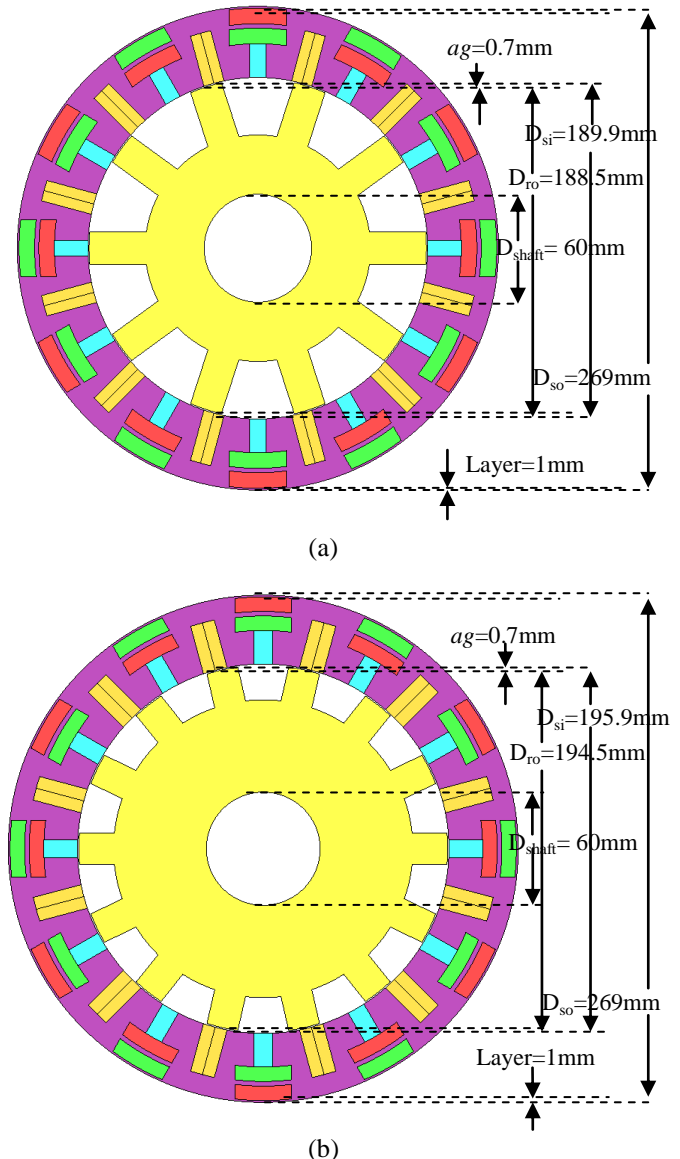


Figure 3: Main machine dimensions of the final design (a) 12-slot 10-pole (b) 12-slot 14-pole



Table 1: Overall performances of final design HEFSM

Items	12S-10P HEFSM	12S-14P HEFSM
PM weight (kg)	1.3kg	1.3kg
Maximum speed (r/min)	20,000	20,000
Maximum torque (Nm)	266.64	304.82
Maximum power (kW)	127.92	133.53
Rotor mechanical stress at 20,000r/min (MPa)	207	236
Machine weight (kg)	35.77	38.11
Maximum torque density (Nm/kg)	7.46	8.01
Maximum power density (kW/kg)	3.55	3.41
Motor efficiency over most of operating region	85%	85%

In this paper, the PM demagnetization of HEFSM and general B-H characteristics are discussed. The demagnetization results for initial and final design are compared. Then, the mitigation process by a few methods is conducted.

PM DEMAGNETIZATION

Introduction of PM Demagnetization

PMs are used in many electrical machines and motors including various BDC motors, synchronous motors, loudspeakers, etc. When subjected to external magnetic fields and/or temperature changes, the magnetic properties of PMs may change, leading to demagnetization, which may affect the performance of such machines. It is therefore very important to take this phenomenon into account when designing such machines.

JMAG-Studio ver.11.0, released by Japanese Research Institute (JRI) is used to design a machine and to study the demagnetization characteristics of machines containing PMs. HEFSM verified the PM effect of increasing machine performances especially torque and power. Demagnetization of PMs generally occur due to factors such as load situations that require high starting torques and fixture reaction that occurs during the rapid change from transient situation to stationary state, magnetic fields in opposite directions that are caused by currents passing through stator coils in static state and high temperature that occur during winding faults [3,4].

Irreversible losses occur as a result of fluxes produced by the magnets which in turn cause decrease in motor efficiency [5]. In addition, vibration and increase in noise are take place due to unbalanced magnetic pull caused by the demagnetization fault. PM demagnetization may occur especially in high loads or due to armature reaction that occurs during the rapid change from permanent situation to static state.

Selection of PM used in this design is also important to negative flux that can eliminate or demagnetize the PM flux. As part of the demagnetization study, the PM temperature is set to 180 degree, 140 degree, 100 degree, 60 degree and 20 degree. Figure 4 illustrates the workflow to

analyze the PM demagnetization The process starts with finding PM demagnetization for initial and final design.

The maximum area of demagnetization and percentages of maximum PM demagnetization are analyzed.

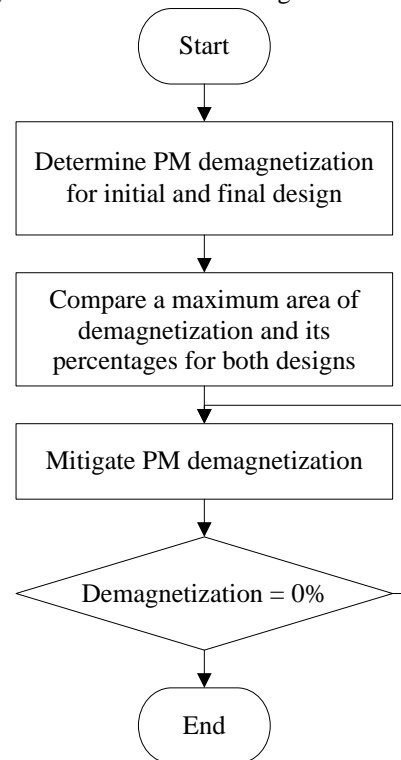


Figure 4: Workflow for PM demagnetization analysis

Since PM demagnetization affected the performances of the machine, mitigation of PM demagnetization is conducted by removing the demagnetization part in PM, and restructuring the PM size to keep the PM volume constant.

General B-H Characteristics

Figure 5 shows the BH curve of the PMs for NEOMAX-35AH materials. The general BH characteristics are divided with three regions which have their own

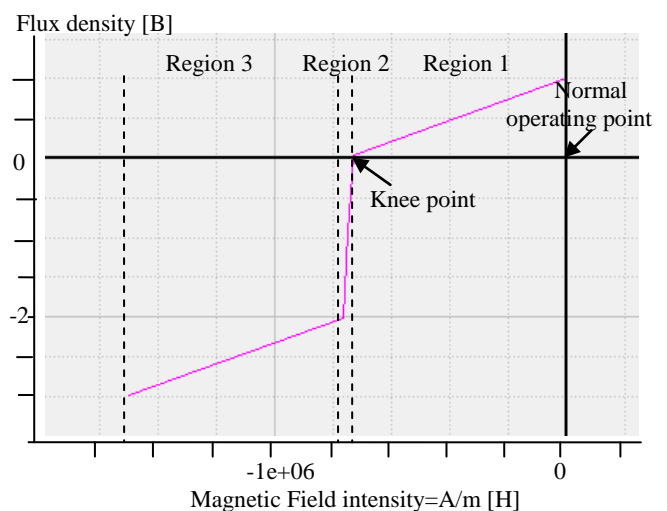


Figure 5: B-H curve



conditions. A region between normal operating point and knee point known as region 1. In this region, a flux operating at normal conditions. Meanwhile, region 2 is region when the flux characteristic is totally differ from their normal operating region. Much higher negative current injected in the machine, the flux characteristics transform to region 3 which is parallel with region 1

Normal operating point can be explained as a point when magnetic density is equal to zero and the flux density is the value at y-axis intersection. Knee point is a point where flux start to change its behavior to be in a new flux characteristics. This point depends on magnetic flux density which are the more negative magnetic flux is injected in machine, the closer to knee point.

The demagnetization curve of the PMs for NEOMAX-35AH material at various temperatures is illustrated in Figure 6. Pink, blue, green, red and black line indicates demagnetization curve at 180°C, 140°C, 100°C, 60°C and 20°C, respectively. Knee point can be referred as base reference for PM demagnetization analysis. The demagnetization curve is depends on temperature, which is at high temperature, the knee point is low as flux density.

From the figure, it is clear that the knee point is different with temperature. As temperature of PMs are increases with time, the knee point of demagnetization curve increases. At high temperature condition as high as 180°C, the demagnetization becomes worst. Other than that, demagnetization curve with various temperatures is

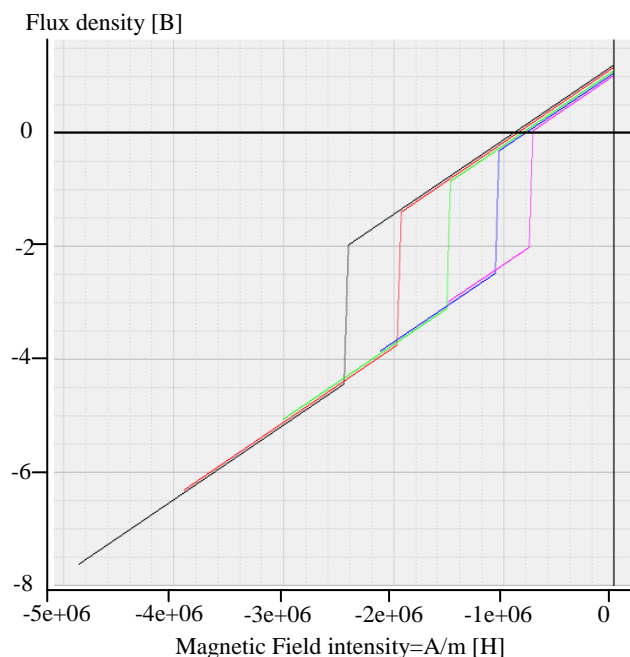


Figure 6: B-H curve at various temperature

referred to identify whether an element of PM is demagnetized or not. Based on B-H characteristic graph, PM flux less than knee point is considered demagnetize.

Maximum Area PM Demagnetization for Initial and Final Design

Selection of PM used in the proposed 12-slot 10-pole and 12-slot-14-pole HEFSM is important to avoid

demagnetization at high temperature. The demagnetization ration of PM in this machine is defined as

$$\%D = \frac{\text{Volume of PM demagnetize}}{\text{Total volume of PM}} \quad (1)$$

To identify whether an element of PM is demagnetized or not, the knee point on the demagnetization curve is referred. From the calculation, the demagnetization value in the PM used in 12-slot-10-pole and 12-slot-14-pole can be investigated.

Investigation an initial and final design 12-slot 10-pole and 12S-14P HEFSMs are conducted to identify the maximum area and percentage of PM demagnetization. All proposed design at this stage has a limitation of operating in various temperature conditions such as 180°C, 140°C, 100°C, 60°C and 20°C due to excessive PM demagnetization. Figure 7 and Figure 8 shows the PM demagnetization at high temperature which is at 180°C for each steps of initial and final design 12S-10P HEFSM, respectively.

Moreover, the PM demagnetization for each step is listed in Table 2 and Table 3. The area of PM demagnetization and its percentage are increased when the step is risen. As the demagnetization of PM in a machine effect its performance, therefore after following various steps of optimization, demagnetization of PM for improved design is reduced from 0.39% to 0.06% which is quite low from initial design. The PM length and PM width is sensitive to the performance of the machine. An increase in PM length will reduce the PM width to kept the same PM volume of 1.3kg. This will extract more flux to flow from the PM because of increase in the stator tooth opening angle will give much space for the flux to flow to the rotor.

However, much longer D4 will cause the PM demagnetization. For final design of 12-slot 10-pole, the PM length is decrease from 26.78mm to 18.78mm.

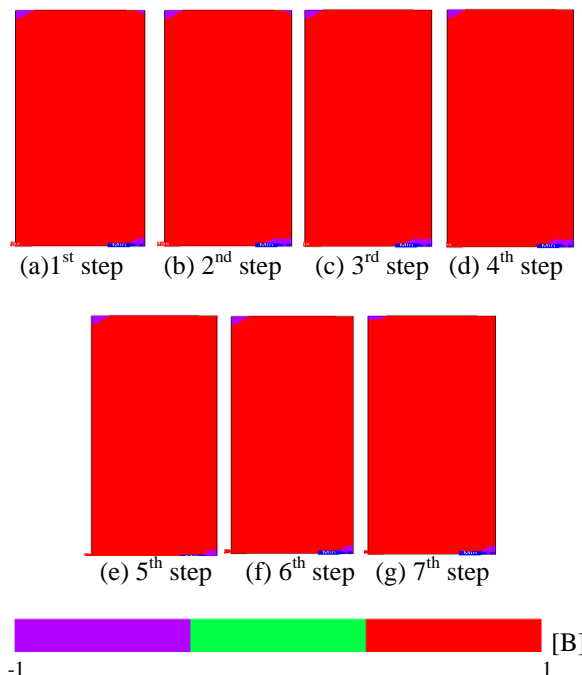


Figure 7: PM demagnetization of initial design 12-slot 10-pole at 180°C

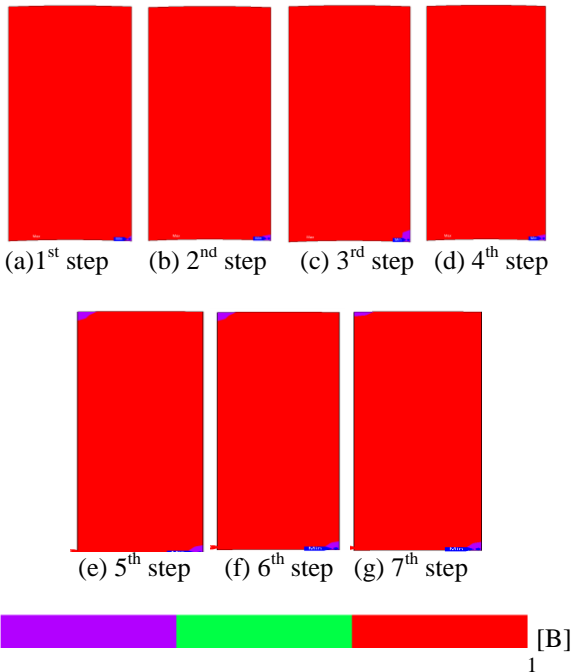


Figure 8 PM demagnetization of final design 12-slot 10-pole at 180°C

Table 2: PM Demagnetization of initial design 12-slot 10-pole

Demagnetization at 180°C			
Total Area		205.04	
Step	Area D	D[%]	T(Nm)
1	0.81	0.39	301.707
2	0.81	0.39	306.486
3	0.81	0.39	312.348
4	0.81	0.39	317.558
5	0.81	0.39	315.922
6	0.81	0.39	300.73
7	0.65	0.32	299.667
		T _{ave}	307.774

Table 3: PM Demagnetization of final design 12-slot 10-pole

Demagnetization at 180°C			
Total Area		170.87	
Step	Area D	D[%]	T(Nm)
1	0.11	0.06	301.707
2	0.11	0.06	306.486
3	0.11	0.06	312.348
4	0.11	0.06	317.558
5	0.11	0.06	315.922
6	0.11	0.06	300.73
7	0.11	0.06	299.667
		T _{ave}	307.774

Therefore, the PM demagnetization is reduced approximately 0.33% from initial design. In addition, the comparison of PM demagnetization for final design in

various temperatures is listed in Table 4. At high temperature, the effect of demagnetization is prominent as can be seen from the table of demagnetization for 12-slot 10-pole, while for other value of temperature, no such demagnetization effect occurs concluding that the machine can be operated under normal temperature.

Table 4: PM Demagnetization of final design 12-slot 10-pole

Temperature (°C)	Max. area demagnetization	Percentage of PM demagnetization
180	0.11	0.06
140	0.00	0.00
100	0.00	0.00
60	0.00	0.00
20	0.00	0.00

Similar to 12-slot 10-pole design, the PM demagnetization at 180° of initial and final design with 12-slot 14-pole configurations are illustrated in Figure 9 and Figure 10, respectively. The PM demagnetization and its percentage of the machine is different when the steps is change as listed in Table 5 and Table 6. Higher PM height will give more space for flow because of increasing stator tooth opening angle that can increase the torque. Although more PM length will increase the flux to flow in the stator body, but there is high possibility of PM demagnetization especially at the edge of PM. The PM volume is set to 1.3kg similar with the previous 12-slot 10-pole HEFSM.

The PM height of initial and final 12-slot 14-pole design are 26.78mm and 17.18mm, respectively. When compare the percentage of PM demagnetization for initial And final design, it is clear that the percentage of final design at high temperature is reduced from 1.97% to 1.65%.

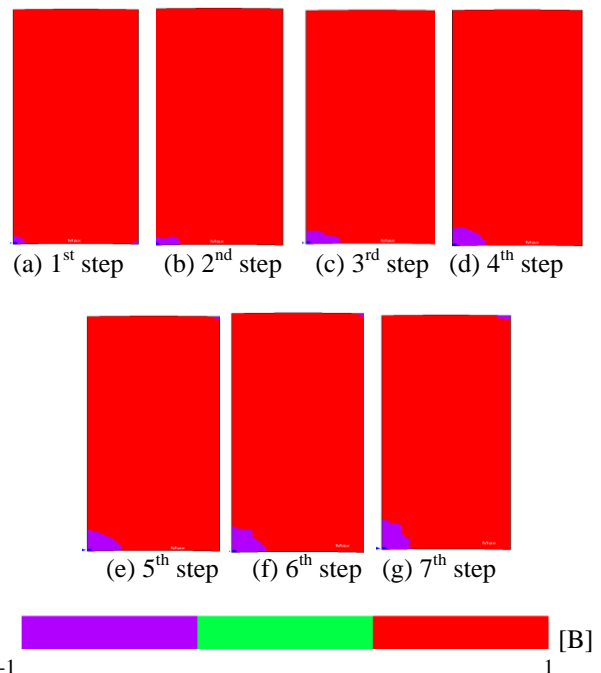


Figure 9: PM demagnetization of initial design 12-slot 14-pole at 180°C

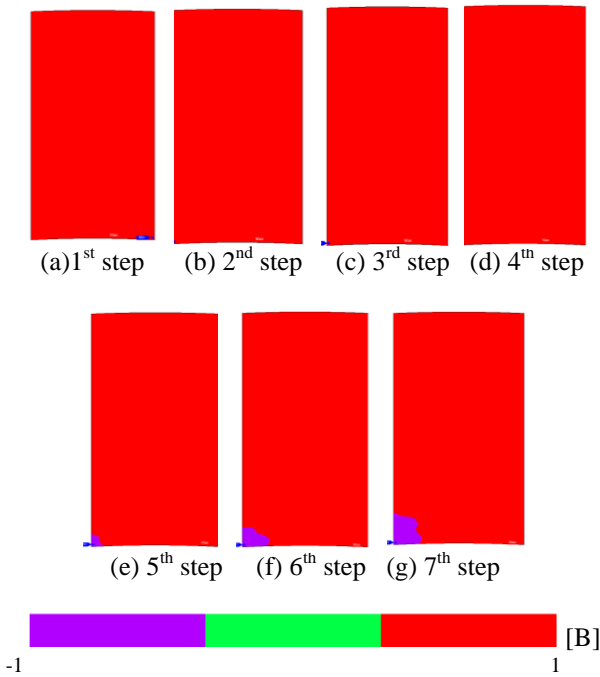


Figure 10: PM demagnetization of final design 12-slot 14-pole at 180°C

Table 5: PM Demagnetization of initial design 12-slot 14-pole

Demagnetization at 180°C			
Total Area		205.04	
Step	Area D	D[%]	T(Nm)
1	0.26	0.13	301.707
2	0.91	0.44	306.486
3	1.82	0.89	312.348
4	2.34	1.14	317.558
5	3.12	1.52	315.922
6	3.51	1.71	300.73
7	4.03	1.97	299.667
		T _{ave}	307.774

Table 6: PM Demagnetization of final design 12-slot 14-pole

Demagnetization at 180°C			
Total Area		170.88	
Step	Area D	D[%]	T(Nm)
1	0.00	0.00	301.707
2	0.00	0.00	306.486
3	0.00	0.00	312.348
4	0.00	0.00	317.558
5	0.22	0.13	315.922
6	1.52	0.89	300.73
7	2.82	1.65	299.667
		T _{ave}	307.774

The final design is much better than the initial design in order to allow the machine to perform better as the demagnetization of PM decreases. Table 7 shows the percentage of PM demagnetization in different temperature.

Table 7: PM Demagnetization of final design 12-slot 10-pole

Temperature (°C)	Max. area demagnetization	Percentage of PM demagnetization
180	2.82	1.65
140	0.94	0.55
100	0.11	0.06
60	0.00	0.00
20	0.00	0.00

From the table, it obvious that there is no PM demagnetization up to 60 °C.

When compare the PM demagnetization of final design with 12-slot 10-pole and 12-slot 14-pole configuration, it is obvious that percentages demagnetization occurs in PM for 12-slot 14-pole design is quite higher compared to 12-slot 10-pole HEFSM. The main reason for this outcome because of the different rotor pole width between both designs. The rotor pole width for design with 12-slot 10-pole and 12-slot 14-pole configuration is 9.06mm and 8.33mm, respectively. Theoretically, 12-slot 14-pole HEFSM with small rotor pole width forced PM flux to flow from stator to rotor and rotor to stator, which results in high pressure in PMs compared to design with wider rotor pole width.

Different in number of rotor poles also effect on maximum PM demagnetization in the machine. For 12-slot 14-pole HEFSM, the flux linkage is higher compared to 12-slot 10-pole HEFSM because of flux completing its cycle in a short distance. Higher generation of flux give a possibility higher demagnetization. Figure 11 shows the flux linkage generatd by PM only of both design. From the figure, it is clear that the flux generated in 12-slot 14-pole design is higher than 12-slot 10-pole design, which is more than 50%. Therefore, a design with 12-slot 14-pole configuration has high PM demagnetization compared to 12-slot 10-pole HEFSM.

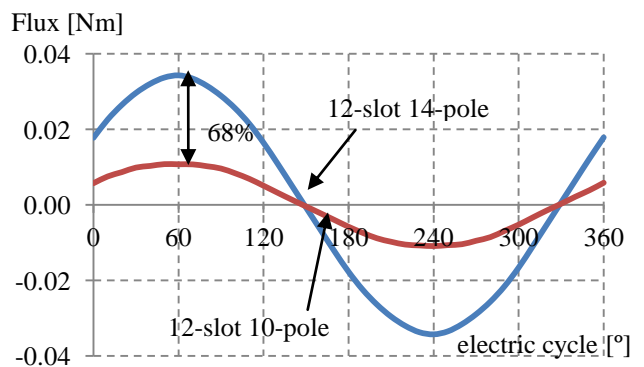


Figure 11: Flux linkage at PM only



Mitigation of PM Demagnetization for 12-slot 10P-pole and 12-slot 14-pole HEFSM

The PM demagnetization and its percentage of final design for both HEFSM is quite low compared to their initial design. But the excessive demagnetization PM as shown in Figure 12 should be removed from the machine until it achieved 0% demagnetization at high temperature of 180°C. The excessive demagnetization occurs at the lower edges of PM and the maximum area demagnetization of 12-slot 10-pole and 12-slot-14-pole reaches as high as 0.11mm² and 1.26mm², respectively.

In order to design a machine with 0% demagnetization, the mitigation process is conducted with kept the same PM volume of 1.3kg. PM demagnetization should be mitigated in the final design of 12-slot 10-pole and 12-slot 14-pole HEFSM by using two methods. The first mitigation method is introduced by increasing the additional air gap between PM and stator inner radius. While, by removing the part that have been magnetized is being a second method of mitigation process on PMs. This method are done by restructured the PM size which is increased the width of the PM while keeping the PM length as constant as before

Distance between air gap and inner PM become very important parameter to avoid PM demagnetization especially if the machine operating in high temperature condition. These parameters can be treated together with the PM width to ensure 0% PM demagnetization at high temperature condition as high as 180°C. The first method to removing demagnetization area for 12-slot 10-pole and 12-slot 14-pole design is by increasing the additional air gap, $H_{air-gap}$ based on the maximum length demagnetization take place as shown in Figure 13.

Furthermore, to ensure that the PM is not demagnetized at temperatures as high as 180°C, the width and the height of excessive demagnetization area are removed with the same PM volume. At this stage, the other parameters are also kept constant. The demagnetization ratio of PM is defined as a volume of PM demagnetized to the total volume of PM. The knee point on demagnetization curve is referred to identify whether an element of PM is demagnetized or not.

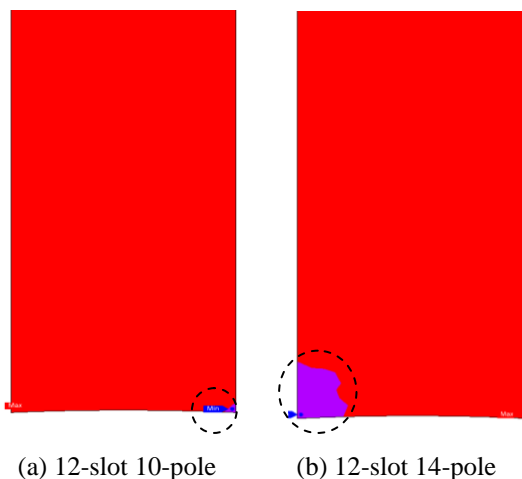


Figure 12: Excessive demagnetization at high temperature

Figure 14 shows the PM condition after removing demagnetization area. For 12-slot 10-pole design, the excessive PM demagnetization is occurred at lower edges

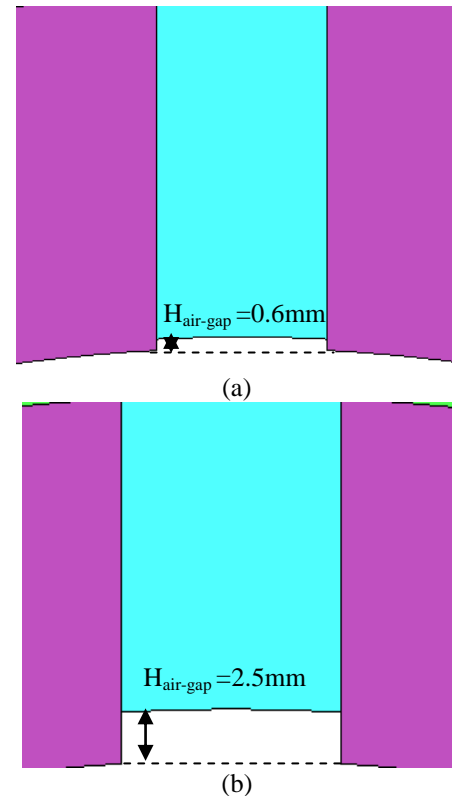


Figure 13: Increasing additional air gap, $H_{air-gap}$

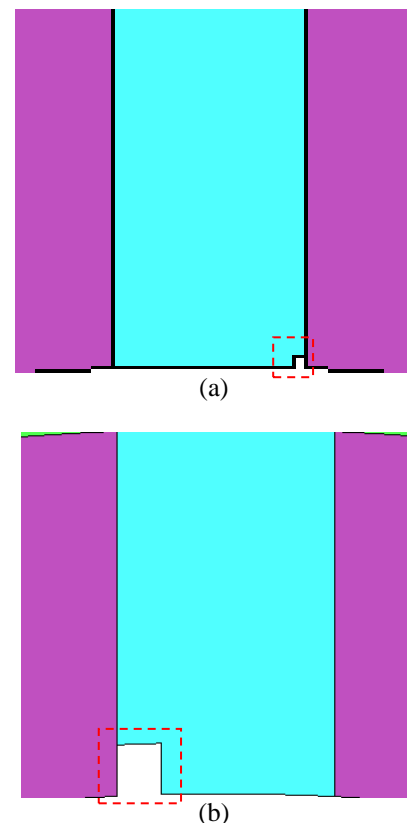


Figure 14: Removing demagnetization area



on the right side with a height and width of 0.6mm and 0.5mm, respectively. Therefore, to fulfill the conditions of adding air gap, 1mm of PM at lower part is reduced and the width of PM is added in order to keep the constant volume of PM. By removing area demagnetization, the areas with 0.5mm×0.6mm is reduced and replace it by adding the PM width. The result of PM demagnetization at 180°C and the performance of torque is listed in Table 8.

Similar with 12S-10P, the previous step is conducted to remove an excessive demagnetization occurs in lower edges on the left side of 12S-14P HEFSM design as listed in Table 9. The first step is conducted by increasing 2.5mm air gap from inner stator diameter to PM. The width and height of demagnetization takes place in 12S-14P design is higher than 12S-10P design with 2.5mm for both width and height should be removed.

The introduction of additional air gap and removing demagnetization area for both design give 0% demagnetization at high temperature but slightly reduce the target performances.

Table 8: Zero demagnetization of 12-slot 10-pole

	Hair-gap	Removing area (Width×Legth)
Parameter reduce	0.6mm	0.5mm×0.6mm
D (%)	0.0	0.0
T (Nm)	230.12	245.64

Table 9: Zero demagnetization of 12-slot 14-pole

	Hair-gap	Removing area (Width×Legth)
Parameter reduce	0.6mm	0.5mm×0.6mm
D (%)	0.0	0.0
T (Nm)	230.12	245.64

CONCLUSION

HEFSM verified the PM effect of increasing machine performances especially torque and power. PM are used in the machine possibly effect on demagnetization when the magnetic properties is changed. In this paper, PM demagnetization of initial and final design 12-slot 10-pole and 12-slot 14-pole HEFSM has been presented and analyzed. Both final 12-slot 10-pole and 12-slot 14-pole configurations achieved maximum PM demagnetization of 0.06% and 1.65% , respectively. Mitigation of PM demagnetization by introducing additional air gap and removing demagnetization area has been proposed in effort to reduce the PM demagnetization. As conclusion, both final design have successfully achieve 0% demagnetization.

ACKNOWLEDGEMENT

This work funded by Research Innovation, Commercialization and Consultancy management (ORICC) with Vot No E15501, Universiti Tun Hussein Onn Malaysia (UTHM) and Ministry of Education Malaysia (MOE).

REFERENCES

- E. Sulaiman, Takashi Kosaka, Nobuyuki Matsui (2011). A Novel Hybrid Excitation Flux Switching Machine for High-speed Hybrid Electric Vehicle Applications, *International Conference on Electrical Machines and System 2011*, pp.1-6, 2011.
- S.K. Rahimi, E. Sulaiman (2014). Design of Hybrid Excitation Flux Switching Machine for High-speed Electric Vehicles, *IEEE 8th International Power Engineering and Optimization Conference, PEOCO 2014*, pp.303-307.
- E. Sulaiman, M. Z. Ahmad, Z.A Haron, and T. Kosak (2012). Design Studies and Performance of HEFSM with Various Slot-pole Combinations for HEV Applications, *IEEE International Conference on Power and Energy (PEcon) 2012*, pp.424-429.
- Y. Amara, L. Vido, M. Gabsi, E. Hoang, M. Lecrivain, and F. Chabot (2006). Hybrid Excitation Synchronous Machines: Energy Efficient Solution for Vehicle Propulsion, *IEEE Vehicle Power and Propulsion Conference, VPPC 06*, pp.1-6.
- C. Zhao, and Y. Yan (2005). A Review of Development of Hybrid Excitation Synchronous Machine, *Proc. of the IEEE International Symposium on Industrial Electronics 2005*, Vol.2, pp.857-862.
- R.L Owen, Z. Q. Zhu and G. W. Jewell (2009). Hybrid Excited Flux-switching PM Machines, *Proc. 13th European Conf. on Power Electronics and Applications, EPE 2009*, pp.1-10.
- E.Sulaiman, T. Kosaka, and N.Matsui (2011). Design Optimization of 12Slot-10Pole Hybrid Excitation Flux Switching Synchronous Machine with 0.4kg PM for Hybrid Electric Vehicles, 8th International Conference on Power Electronics, ECCE Asia, pp 1913-1920.

